

Local reactivity of metal overlayers

Ata Roudgar and Axel Groß

Physik-Department T30, Technische Universität München, James-Frank-Str., 85747 Garching, Germany

(Dated: November 8, 2002)

The local reactivity of Pd overlayers supported by Au has been studied by calculating atomic hydrogen and CO adsorption energies as a microscopic probe. The calculations are based on density functional theory within the generalized gradient approximation. The binding energies show a maximum on two Pd layers on Au, both for the (100) and (111) surfaces. We have furthermore analysed local trends by considering different adsorption sites on the Pd overlayers. The results can be rationalized within the d -band model if also second-nearest neighbor interactions and bond-length effects are taken into account.

PACS numbers: 68.43.Bc, 68.47.De, 82.65.+r

The systematic modification of the reactivity of metal surfaces is of strong current interest since it might lead to the design of better catalysts in heterogeneous and electro-catalysis [1]. In particular, bimetallic surfaces are well-suited for the tailoring of reactivity properties [2–6] since they offer the possibility to prepare specific surface compositions and structures. If a thin film of one metal is deposited pseudomorphically on another metal with a different lattice constant, strained metallic overlayers result. Substrate strain can strongly modify the surface reactivity, as has recently been shown experimentally [7, 8]. These findings have been rationalized [9] within the d -band model [10]. The modified overlap between the substrate atoms at a strained transition metal surface causes a shift of the d -band thus changing the reactivity.

In the case of metallic overlayers, in addition to the pure strain effect, also the change in the electronic structure of the thin film due to the interaction with the underlying support has to be taken into account [11, 12]. The strength of this interaction is not well-understood yet. While it is almost impossible to disentangle the consequences of these different effects in experiment, electronic structure calculations provide an excellent means to elucidate the underlying microscopic mechanisms [13] when properly chosen systems are compared.

In this letter, we report a theoretical study of the local reactivity of up to three Pd overlayers on Au(111) and Au(100) based on density functional theory (DFT). We have used atomic hydrogen and CO adsorption energies as a local probe in order to determine the trends in the reactivity. The system Pd/Au is of particular interest in the field of electrocatalysis [14–18] because of its catalytic activities in the oxidation reactions of methanol, formic acid and carbon monoxide. At the same time, it is a prototype system for the study of the reactivity of strained overlayers. Gold as a noble metal acts as an almost inert support. The lattice constant of Au, $a_{\text{Au}} = 4.08 \text{ \AA}$, is 5% larger than the lattice constant of Pd, $a_{\text{Pd}} = 3.88 \text{ \AA}$ which means that the Pd overlayers on Au are expanded by 5%. Still up to 10 monolayers of Pd can grow pseudomorphically on Au(100) [16, 19] and Au(111) [15, 20].

The considered high-symmetry hydrogen adsorption sites on a Pd two-layer film supported by an Au(100)

slab are illustrated in Fig. 1. Our calculations show that in general the binding energies on the Pd/Au-overlayers are larger than on pure Pd substrates. We find maximum binding energies for two Pd layers on Au. These results can be rationalized within the d -band model [9, 10], but only if also second-nearest neighbor interactions are taken into account. To understand the local variation in the strain effects on the adsorption energies, additionally the modification of the adsorbate-substrate bond length has to be taken into account.

The DFT calculations have been performed using the Vienna *ab initio* simulation package (VASP) [21]. The exchange-correlation effects are described within the generalized gradient approximation (GGA) using the Perdew-Wang (PW-91) functional [22]. Due to the use of ultrasoft pseudopotentials [23] as constructed by G. Kresse and J. Hafner [24], cut-off energies of 200 eV for hydrogen adsorption and 400 eV for CO adsorption were sufficient to obtain converged total energies. Throughout the study we used the calculated equilibrium lattice constants for bulk Pd and Au, 3.96 Å and 4.18 Å, respectively, which are in good agreement with the experiment (3.88 Å and 4.08 Å, respectively).

The Pd/Au overlayer structure is modelled by a slab of five layers of Au on which up to three Pd layers have been

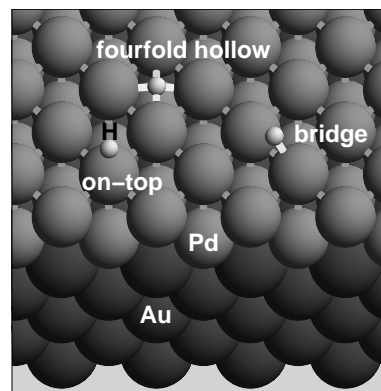


FIG. 1: Considered hydrogen adsorption sites on a two-layer thick pseudomorphous Pd film on a five-layer slab of Au(100).

deposited. All layer structures are separated by 14 Å of vacuum. The three bottom layers of the slabs have been kept fixed at their corresponding bulk positions, while all upper layers including the overlayers have been fully relaxed. All adsorption energies reported in this letter have been obtained for an coverage of $\Theta = 0.25$ in (2×2) surface unit cells. We used a Monkhorst-Pack \mathbf{k} -point set of $7 \times 7 \times 1$, corresponding to 8 \mathbf{k} -points in the irreducible Brillouin zone. For the analysis of the electronic structure, we used a finer mesh of $11 \times 11 \times 1$ \mathbf{k} -points, corresponding to 16 \mathbf{k} -points in the irreducible Brillouin zone. We have carefully checked that our results are converged with respect to these numerical parameters. In order to disentangle the pure strain effect from the interaction with the metal support, we also performed calculations for pure Pd slabs with the intrinsic Pd lattice constant a_{Pd} and with the Au lattice constant a_{Au} . The results corresponding to the expanded pure Pd surface are denoted by Pd@Au in the following.

The hydrogen adsorption energies are determined via

$$E_{\text{ads}}(\text{H}) = E_{\text{slab}+\text{H}} - \left(E_{\text{slab}} + \frac{1}{2} E_{\text{H}_2} \right), \quad (1)$$

where E_{slab} and $E_{\text{slab}+\text{H}}$ are the total energies of the slab without and with the adsorbed hydrogen. For the H_2 binding energy E_{H_2} in the gas phase the calculated GGA value is taken. Since CO adsorbs molecularly, its adsorption energy is given by $E_{\text{ads}}(\text{CO}) = E_{\text{slab}+\text{CO}} - (E_{\text{slab}} + E_{\text{CO}})$. The energy gain upon adsorption is reflected by a negative adsorption energy, therefore binding energies are defined as negative adsorption energies.

The calculated adsorption energies as a function of the number of Pd overlayers on Au(111) and Au(100) for different high-symmetry adsorption sites are collected in Fig. 2. It is striking that we find the same trends for CO and H adsorption in spite of their different electronic structure. For both adsorbates, the binding energies on thin Pd/Au overlayers are larger by up to 0.2–0.3 eV than on pure Pd substrates and show their maximum for two Pd overlayers at all considered adsorption sites. At the most densely packed (111) surface, the adsorption energies on three Pd overlayers are almost the same as on the pure expanded Pd slabs. This means that the electronic effect of the underlying Au substrate only contributes significantly to the reactivity of the first two overlayers, from the third layer on the modified reactivity is dominated by geometric effect caused by the lattice expansion. For the less densely packed (100) surface that has a smaller layer spacing, there is still some influence of the Au support up to the third Pd overlayer. Note that our results are in agreement with experiments which find a strongly modified activity of Pd films deposited on Au as a function of the film thickness for one to three Pd overlayers [14, 17].

In order to understand the trends in the adsorption energies as a function of layer thickness, we have utilized the d -band model as proposed by Hammer and Nørskov [10]. Since CO and hydrogen show the same trends in the adsorption energies, we will concentrate on hydro-

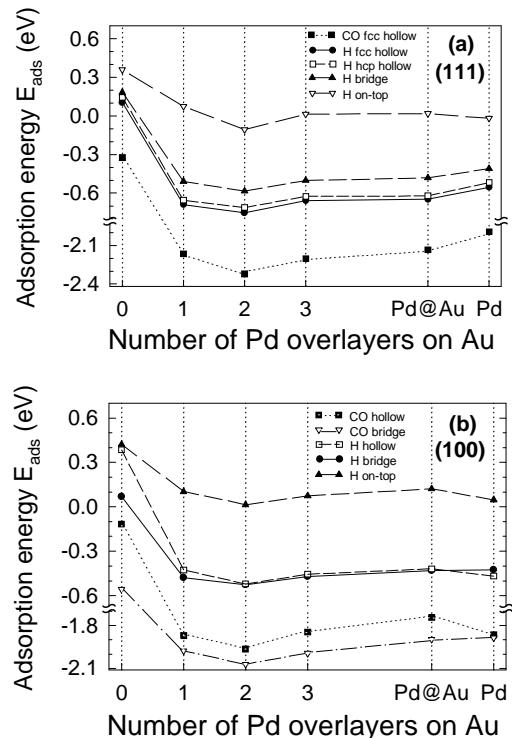


FIG. 2: CO and hydrogen adsorption energies as a function of the number of Pd overlayers on Au for different adsorption sites on the (111) (a) and the (100) surface (b) at an coverage of $\theta = 0.25$. The pure Pd substrates with the lateral lattice constant of Au ($a = 4.18$ Å) and Pd ($a = 3.96$ Å) are labeled by Pd@Au and Pd, respectively.

gen adsorption in our analysis of the electronic factors determining the reactivity in the following. In the d -band model, the interaction between an adsorbate and a transition or noble metal is formally split into a contribution arising from the s and p states of the metal and a second contribution coming from the d -band. The interaction with the sp -bands is assumed to lead to an energy renormalization of the adsorbate energy levels. According to the d -band model, there is a linear relationship between the d -band center shift ϵ_d and the change in the chemisorption strength δE_d on metal surfaces [25, 26],

$$\delta E_d = - \frac{V^2}{|\epsilon_d - \epsilon_a|^2} \delta \epsilon_d. \quad (2)$$

Here ϵ_a is the renormalized adsorbate resonance and ϵ_d is the center of the local d -band at the position of the substrate atom. The coupling matrix element V depends on the distance between the interacting atoms and usually decreases rapidly with increasing distance [10]. If the adsorbate is interacting with nonequivalent substrate atoms, then the right-hand side of eq. 2 has to be replaced by the corresponding sum over these atoms.

According to eq. 2, an upshift of the Pd d -band is associated with a stronger interaction. If the d -band is more than half-filled, a lattice expansion or a reduced coordina-

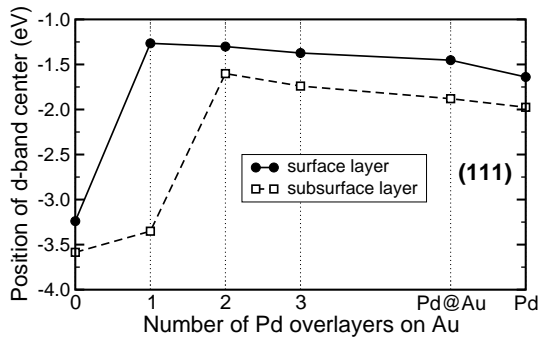


FIG. 3: Position of the local center of the d -band with respect to the Fermi energy as a function of the number of Pd overlayers on Au(111) for the surface and the subsurface layer. The overlayers are labelled in the same way as in Fig. 2.

tion leads to a smaller d -bandwidth and to an upshift of the d -band due to charge conservation [9, 27]. This effect explains for example the preferential adsorption of hydrogen at the step atoms of the Pd(210) surface [28, 29].

In Fig. 3 the position of the d -band center is plotted as a function of the number of Pd overlayers on Au(111) for the uppermost and the subsurface layer. The results for the (100) surfaces look very similar. Comparing the data for pure Pd and Pd@Au, it is obvious that expanding the Pd substrate to the Au lattice constant leads to a significant upshift of the d -band center. However, in addition to this geometric effect, the electronic interaction of Pd with the underlying Au substrate leads to a further upshift of the Pd d -band. This can in fact be understood by the inertness of the Au substrate. Our calculations show that Pd atoms are less strongly bound to Au than to Pd which means that effectively a Pd overlayer has less overlap with an underlying Au substrate causing a band narrowing and upshift. On the basis of our findings we thus propose that depositing a reactive metal on an inert metal with a larger lattice constant should in general lead to a higher reactivity of the overlayer. Exactly the opposite trend we expect for an overlayer of a less reactive metal on a more reactive metal with a smaller lattice constant, such as, e.g., Pt on Ru [30].

Still the analysis of the top-layer density of states does not explain why the binding energies show a maximum on two Pd overlayers on Au. In fact, we find the highest d -band center for one Pd overlayer which should consequently be the most reactive structure. However, the difference in the hydrogen adsorption energies between the fcc and the hcp positions on Pd(111) indicates that the second layer plays an important role for the adsorption because the fcc and hcp sites only differ in the second-nearest neighbors in the subsurface layer. Fig. 4 shows the charge density difference induced upon hydrogen adsorption at the on-top position of two Pd overlayers on Au(111). There is a sizable charge arrangement at the second layer atom which, however, is caused indirectly by the adsorbate. This is confirmed by an analysis of the local density of states at the second layer Pd atom, which

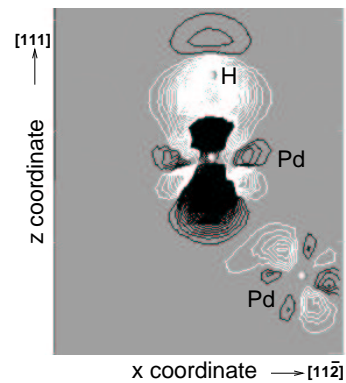


FIG. 4: Charge density difference plot for hydrogen adsorption at the on-top position of two Pd overlayers on Au(111). White contours correspond to charge accumulation while black contours denote charge depletion.

shows no hybridization with the H $1s$ state but a modified coupling to the first layer Pd atom upon H adsorption. Similar results are found at all other adsorption sites. In terms of the d -band model, it is therefore important to consider the d -band centers in the subsurface layers that are also included in Fig. 3. For one Pd overlayer, this subsurface layer corresponds to the topmost Au layer. Gold has a very deep lying filled d -band which makes it to an inert noble metal [31]. It is thus the indirect interaction of the adsorbate with the inert Au substrate beneath the one-layer thick Pd film that leads to a weaker binding compared to the two-layer thick Pd film.

Now we would like to concentrate on the pure strain effects on Pd surfaces. On Ru(0001), DFT calculations have found a surface reactivity increasing with lattice expansion, as far as O and CO adsorption energies and the CO dissociation barrier are concerned [9]. In our calculations, on the other hand, we do not obtain a unique trend of the adsorption energies as a function of the lattice expansion. While the binding energies at the threefold hollow and the bridge position on the Pd(111) surface increase with lattice expansion, they decrease at the top position of both the (100) and (111) surface and at the fourfold hollow position of Pd(100).

A lattice expansion does not only cause a reduced overlap between the substrate atoms, it could also lead to an extension of the adsorbate-substrate bond which would result in a weaker interaction. However, at the bridge and the threefold-coordinated hollow positions the hydrogen atom can keep its optimum bond length by simply relaxing towards the surface. Upon expanding the lateral lattice constant of the Pd(111) surface by 5%, the hydrogen adsorption height is reduced from 0.97 Å to 0.86 Å at the bridge site and from 0.84 Å to 0.62 Å at the threefold hollow position, thus keeping the H-Pd distances to the nearest neighbors constant within ± 0.01 Å.

At the fourfold hollow position of the (100) position, however, this mechanism can not work any longer. This is due to the fact that at the minimum energy position

the hydrogen atom sits rather deep in the first Pd surface layer only 0.32 Å higher than the Pd atoms. This configuration is illustrated in Fig. 1. Although the hydrogen atom reduces its height to 0.14 Å upon the lattice expansion and the neighboring Pd atoms also relax towards the hydrogen atom, still the H-Pd bond length increases from 1.99 Å to 2.06 Å. The reduced H-Pd interaction and the energetic cost of the Pd atom relaxations even overcompensate the increase in the reactivity of the expanded surface due to the *d*-band center upshift. As a result, the fourfold hollow and the bridge site become energetically degenerate (see Fig. 2).

Interestingly enough, for hydrogen on one Pd layer on-top of the Au substrate the twofold coordinated bridge site is favored by 50 meV compared to the fourfold hollow site. The hollow site becomes so unfavorable simply because the hydrogen atom is interacting with the inert Au atom directly beneath in the second layer. This causes an effective repulsion that leads to an increase of the hydrogen adsorption height from 0.1 Å to 0.4 Å. As for the hydrogen adsorption on pure Au, the preference for highly coordinated sites is much less pronounced than on Pd. For Au(100), the twofold coordinated bridge site becomes even more favorable by 0.3 eV for hydrogen adsorption compared to the fourfold hollow site.

CO adsorbs preferentially at the bridge site of Pd(100) on the clean unstrained surface [32]. Our calculations indicate that already on pure Pd the reduced distance to the rather inert second layer substrate atom upon lat-

tice expansion is energetically unfavorable. Therefore the difference between bridge and hollow adsorption energies is not further increased by reducing the number of Pd overlayers on Au(100) from two to one (see Fig. 2b).

The hydrogen adsorption energies on the on-top positions of Pd(100) and Pd(111) also show the opposite trend upon lattice expansion than expected from the *d*-band shift. At the top site, for symmetry reasons the hydrogen atom is mainly interacting with only one *d*-orbital of the Pd atom directly beneath, namely the $d_{3z^2-r^2}$ orbital. An analysis of the electronic structure reveals that this interaction is so strong that the *d*-band model is no longer fully appropriate. Instead, the response of the local *d*-band to the presence of the adsorbate has to be taken into account which stabilizes the adsorption at the top site of the compressed surfaces. The same mechanism is also operative in the H/Cu system [33].

In conclusion, we have shown that the local reactivity of metal overlayers is strongly influenced by a combination of strain, metal-support interaction and bond length effects. Our results suggest that the microscopic knowledge of these factors can be used to tailor the activity of catalysts by an appropriate preparation of bimetallic overlayer systems.

Financial support by the Deutsche Forschungsgemeinschaft through the priority program SPP 1030 is gratefully acknowledged. We would like to thank R. Hiesgen, J. Meier, H. Kleine and U. Stimming for stimulating discussions in the course of this work.

-
- [1] F. Zaera, *Surf. Sci.* **500**, 947 (2002).
 [2] J. A. Rodriguez and D. W. Goodman, *Science* **257**, 897 (1992).
 [3] A. P. J. Jansen and C. G. M. Hermse, *Phys. Rev. Lett.* **83**, 3673 (1999).
 [4] K. A. Friedrich, F. Henglein, U. Stimming, and W. Unkauf, *Electrochim. Acta* **45**, 3283 (2000).
 [5] Y. Gauthier *et al.*, *Phys. Rev. Lett.* **87**, 036103 (2001).
 [6] J. H. Sinfelt, *Surf. Sci.* **500**, 923 (2002).
 [7] M. Gsell, P. Jakob, and D. Menzel, *Science* **280**, 717 (1998).
 [8] P. Jakob, M. Gsell, and D. Menzel, *J. Chem. Phys.* **114**, 10075 (2001).
 [9] M. Mavrikakis, B. Hammer, and J. K. Nørskov, *Phys. Rev. Lett.* **81**, 2819 (1998).
 [10] B. Hammer and J. K. Nørskov, *Surf. Sci.* **343**, 211 (1995).
 [11] B. Hammer, *Phys. Rev. Lett.* **89**, 016102 (2002).
 [12] A. Bogicevic and D. R. Jennison, *Phys. Rev. Lett.* **82**, 4050 (1999).
 [13] A. Groß, *Surf. Sci.* **500**, 347 (2002).
 [14] M. Baldauf and D. M. Kolb, *J. Phys. Chem.* **100**, 11375 (1996).
 [15] L. A. Kibler, M. Kleinert, R. Randler, and D. M. Kolb, *Surf. Sci.* **443**, 19 (1999).
 [16] L. A. Kibler, M. Kleinert, and D. M. Kolb, *Surf. Sci.* **461**, 155 (2000).
 [17] H. Naohara, S. Ye, and K. Uosaki, *J. Electroanal. Chem.* **500**, 435 (2001).
 [18] F. Maroun, F. Ozanam, O. M. Magnussen, and R. J. Behm, *Science* **293**, 1811 (2002).
 [19] C. Liu and S. D. Bader, *Phys. Rev. B* **44**, 12062 (1991).
 [20] M. Takahashi *et al.*, *Surf. Sci.* **461**, 213 (2000).
 [21] G. Kresse and J. Furthmüller, *Phys. Rev. B* **54**, 11169 (1996).
 [22] J. P. Perdew *et al.*, *Phys. Rev. B* **46**, 6671 (1992).
 [23] D. Vanderbilt, *Phys. Rev. B* **41**, 7892 (1990).
 [24] G. Kresse and J. Hafner, *J. Phys.: Condens. Matter* **6**, 8245 (1994).
 [25] B. Hammer, O. H. Nielsen, and J. K. Nørskov, *Catal. Lett.* **46**, 31 (1997).
 [26] V. Pallassana, M. Neurock, L. B. Hansen, B. Hammer, and J. K. Nørskov, *Phys. Rev. B* **60**, 6146 (1999).
 [27] A. Ruban, B. Hammer, P. Stoltze, H. L. Skriver, and J. K. Nørskov, *J. Mol. Catal. A* **115**, 421 (1997).
 [28] M. Lischka and A. Groß, *Phys. Rev. B* **65**, 075420 (2002).
 [29] P. K. Schmidt, K. Christmann, G. Kresse, J. Hafner, M. Lischka, and A. Groß, *Phys. Rev. Lett.* **87**, 096103 (2001).
 [30] A. Schlapka, U. Käsberger, D. Menzel, and P. Jakob, *Surf. Sci.* **502**, 129 (2002).
 [31] B. Hammer and J. K. Nørskov, *Nature* **376**, 238 (1995).
 [32] A. Eichler and J. Hafner, *Phys. Rev. B* **57**, 10110 (1998).
 [33] S. Sakong and A. Groß, *subm. to Surf. Sci.*